Supplementary Information for:

The right posterior parietal cortex mediates spatial reorienting of attentional choice bias

Ankita Sengupta, Sanjna Banerjee, Suhas Ganesh, Shrey Grover, Devarajan Sridharan

Correspondence to: sridhar@iisc.ac.in

This PDF file includes:

Supplementary Results
Figures S1 to S9
Table S1

Supplementary Information: Results

Accounting for inter-individual differences in performance

The change angle at which neurostimulation would induce the strongest effect on d' could not be ascertained *a priori*. Therefore, for each participant, we measured the entire psychophysical function across a range of change angles (Δθ, see Figs. 2a, 4a and Supplementary Fig. S4). This produced significant variations in hit rates and false alarm rates across participants. Given this inter-individual variability in performance, we performed the following control analysis.

We normalized the attentional modulation of each psychophysical parameter (Δd', Δc) for each participant by dividing each value by the respective average d' during the sham session; we term this quantity the modulation index (MI). For example, MI (d'_{stim}) = $\Delta d'_{stim}$ / $\langle d'_{sham} \rangle$ where $\Delta d'_{stim} = d'_{cued, stim} - d'_{uncued, stim}$, and $\langle d'_{sham} \rangle = (d'_{cued, sham} + d'_{uncued, sham}) / 2$, i.e., the average d' for the sham session. With this metric, we observed a statistically significant effect of stimulation, again, only on the attentional modulation of criterion (MI(c), cTBS: sham = -0.98±0.30, stim = -1.18±0.26; δ_Δ (stim-sham): z=-2.57, p=0.010, signed rank test, Cohen's d=0.52, CI=[-0.44, 0.03]; tACS: sham = -0.33±0.07, stim = -0.42±0.07; δ_Δ: z=-2.30, p=0.022, Cohen's d=0.57, CI=[-0.18, 0.00]; MI(d'), cTBS: sham = 0.45±0.11, stim = 0.43±0.11; δ_Δ: z=0.36, p=0.716, Cohen's d=0.04, CI=[-0.26, 0.23]; tACS: sham = 0.58±0.07, stim = 0.76±0.11; δ_Δ: z=1.69, p=0.091, Cohen's d=0.54, CI=[-0.02, 0.38]). Taken together, these control analyses indicate that inter-individual variability in performance could not account for the observed effects of cTBS or tACS neurostimulation.

Additional control analyses for training and session order effects

For the cTBS experiment, sham and actual stimulation sessions were conducted on the same day, typically separated by >60 min, in counterbalanced order across all participants (n=28). Because the order was perfectly counterbalanced, there was no reason to expect systematic

training or familiarity effects to influence the cTBS results. ANOVA analysis confirmed this expectation: a two-way ANOVA to compare the effects of stimulation order ('sham first', 'stim first') and stimulation condition (sham, stim) on the attentional modulation of sensitivity (Δd') and criterion (Δc) revealed no statistically significant main effect of stimulation order (Δd': $F_{1,52}$=0, p=0.975, Δc: $F_{1,52}$=1.03, p=0.316), nor a significant interaction between stimulation order and stimulation condition (Δd': $F_{1,52}$=0, p=0.962, Δc: $F_{1,52}$=0.02, p=0.875) on either d' or criterion modulation. Following this, cTBS data were pooled across the cohort of participants regardless of stimulation order.

Participants (n=26) who underwent right PPC tACS stimulation also underwent left PPC tACS stimulation, albeit with a 4x1 electrode montage mirrored relative to the rPPC configuration about the sagittal plane of the head. These sessions were separated by at least one week, and the order of lPPC and rPPC tACS sessions was counterbalanced across subjects. To control for training effects in this case, we performed a two-way ANOVA with stimulation session order ('left PPC first', 'right PPC first') and stimulation condition (sham, stim). This analysis revealed no statistically significant main effect of stimulation session order (Δd': $F_{1,48}$=0.32, p=0.576, Δc: $F_{1,48}$=0.29, p=0.593), nor a significant interaction between stimulation session order and stimulation condition (Δd': $F_{1,48}$=0, p=0.970, Δc: $F_{1,48}$=0.33, p=0.571) on either d' or criterion modulation.

Analysis with a similarity choice model

To lend concurrent validity to these results, we analyzed our behavioral contingency tables with a Similarity Choice model, which is a multialternative decision model that estimates sensitivity and bias based on a factoring of the response proportions (Cane and Luce, 2006). This model also revealed virtually identical estimates of criteria and sensitivity in both the cTBS and tACS experiments. The correlation between parameters across models is presented below:

Δd': cTBS sham: ρ = 0.823, p<0.001; stim: ρ = 0.890, p<0.001; tACS sham: ρ = 0.644, p<0.001; stim: ρ = 0.825, p<0.001

Δc: cTBS sham: ρ = 0.977, p<0.001; stim: ρ = 0.980, p<0.001; tACS sham: ρ = 0.946, p<0.001; stim: ρ = 0.973, p<0.001

Effects of neurostimulation on mislocalization rates

To further analyze the precise effects of neurostimulation, we show the average stimulus-response contingency table (Supplementary Table S1) both before and following neurostimulation. Each cell denotes the percentage (mean ± s.e.m.) of responses for each stimulus event type (cued change, uncued change, no change) pooled across both cohorts, such that response percentages in each row sum to 100%.

Following stimulation, in addition to a decrease in hit rates at the uncued location (green), there was an increase in the proportion of cued mislocalization responses, in which participants reported a change at the cued location on 'uncued change' trials (red). By contrast, there was a decrease in the proportion of the uncued mislocalizations, in which participants reported a change at the uncued location on 'cued change' trials (magenta). There was also a slight increase in false-alarm rates at the uncued location following stimulation (blue). The change in mislocalization responses underlie the increase in m-ADC model criterion at the uncued location – representing a reduction in bias for the uncued location – following stimulation.

We quantified the change in mislocalization rates (MLR), and their modulation, for both neurostimulation cohorts separately. rPPC cTBS did not produce a statistically significant change in mislocalization rates at either the cued or the uncued location (cued: MLR-sham = 29.5±2.6%, MLR-stim = 33.7±3.1%; δ_{cued}: z=1.73, p=0.083, Cohen's d=0.50, CI=[-0.5, 9.0]%; uncued: MLR-sham = 10.5±1.3%, MLR-stim = 9.2±1.3%; δ_{uncued}: z=-1.50, p=0.133, Cohen's

d=0.53, CI=[-2.8, 0.1]%). On the other hand, 40-Hz tACS over the rPPC produced a statistically significant decrease in the mislocalization rates at the uncued location (MLR-sham = 8.1±1.0%, MLR-stim = 6.1±0.9%; δ_{uncued}: z=-3.39, p<0.001, Cohen's d=1.08, CI=[-3.2, -1.0]%), but not at the cued location (MLR-sham = 12.1±1.7%, MLR-stim = 13.5±1.8%; δ_{cued}: z=1.08, p=0.280, Cohen's d=0.39, CI=[-0.7, 3.5]%). Yet both paradigms produced consistent effects on the attentional modulation of mislocalization rates – quantified as the difference in MLR between the cued and uncued locations ($\Delta MLR = MLR_{cued} - MLR_{uncued}$). ΔMLR increased statistically significantly following cTBS (ΔMLR-sham = 18.9±3.3%, ΔMLR-stim = 24.5±3.4%; δ_{Δ}: z=2.00, p=0.045, Cohen's d=0.61, CI=[0.6, 10.6]%) as well as following 40-Hz tACS (ΔMLR-sham = 3.9±1.6%, ΔMLR-stim = 7.4±1.6%; δ_{Δ}: z=2.83, p=0.005, Cohen's d=0.92, CI=[1.3, 5.7]%).

We further highlight the close link between the effect of neurostimulation on m-ADC model parameters and participants' mislocalization responses, with the following analysis: In conventional, one dimensional SDT, the criterion is calculated as: $c = -[\Phi^{-1}(HR) + \Phi^{-1}(FAR)]/2$; where HR is the hit rate, and FAR is the false alarm rate. In other words, the criterion is inversely correlated with the sum of the probits of the hit and false alarm rates. Yet, such a closed form solution does not exist for the m-ADC (multidimensional SDT) model. Nevertheless, to provide intuition, we plot the change in criterion between sham and stimulation sessions ($\delta c = c_{stim} - c_{sham}$), against the change in the sum of the hit rate (HR), false alarm rate (FAR), and mislocalization rates (MLR) across these sessions ($\delta[HR+FAR+MLR] = [HR+FAR+MLR]_{stim} - [HR+FAR+MLR]_{sham}$) (Supplementary Fig. S5). We observed a robust inverse correlation between criterion change following stimulation and the change in the summed HR, FAR, and MLR at each location. Note that only the stimulation-induced change in the uncued criterion (δc), but not sensitivity (δd'), was statistically significantly different from zero across participants, as reported in the Results.

Supplementary Information: Figures

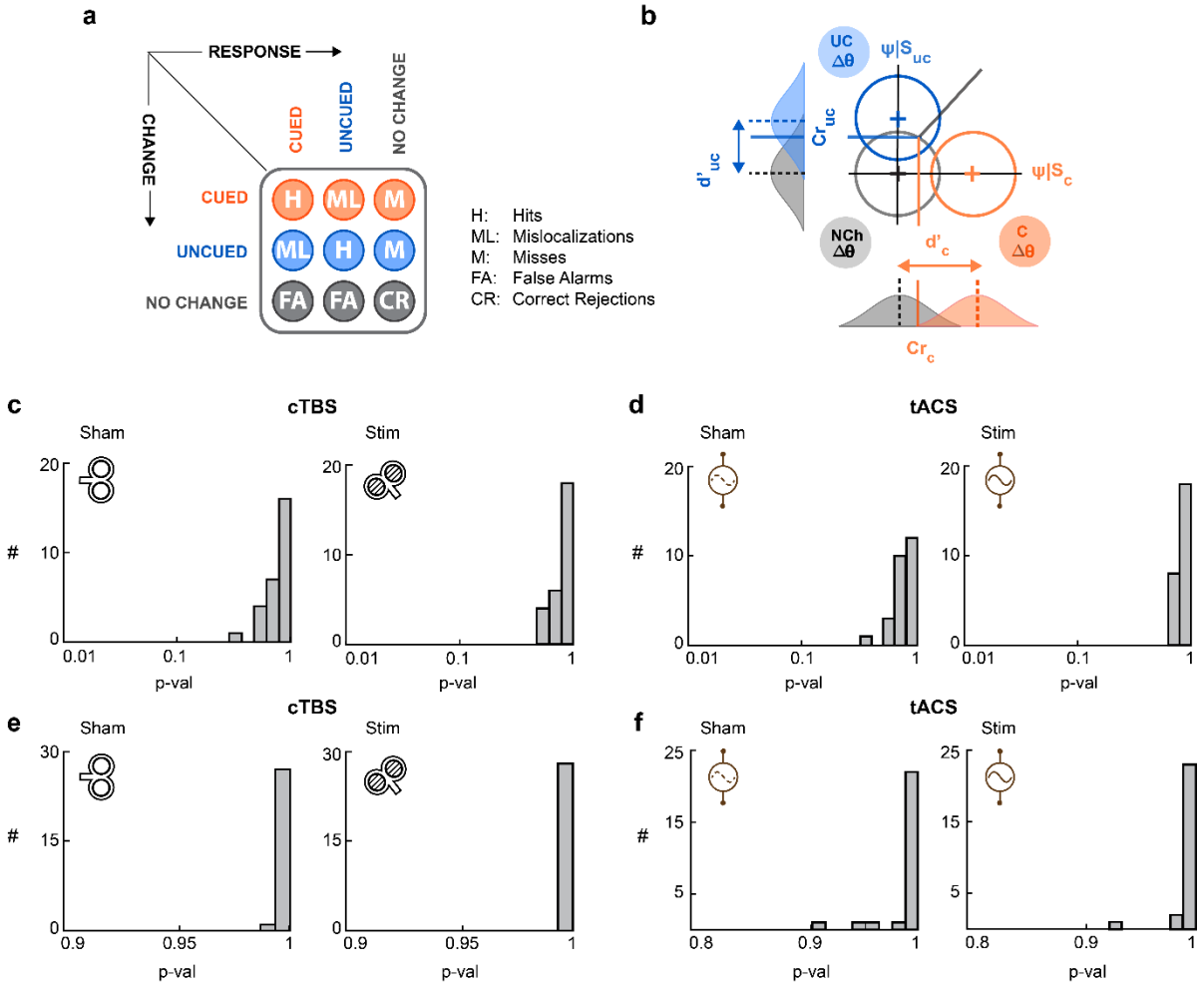

Supplementary Figure S1. Attention task contingency table, model schematic and goodness-of-fit tests. **a.** Schematic of a 3x3 stimulus response contingency table obtained for the cued, endogenous attention task. Rows represent the locations of change (or no change) and columns represent the locations of responses. H: Hits, ML: Mislocalizations, M: Misses, FA: False Alarms, CR: Correct Rejections. **b.** Schematic of a 2-dimensional signal detection (m-ADC, m=2) model for estimating sensitivity and bias in the attention task, by fitting responses in the contingency tables in panel (a). Orthogonal axes represent signal evidence at each location (x axis: cued; y axis: uncued). Circles represent bivariate Gaussian distributions of decision variable (ψ) for changes at the cued (orange, C) and uncued (blue, UC) locations, and for no change (grey, NCh). Grey lines represent decision boundaries that divide the decision space into three decision zones: change at cued location (orange), uncued location (blue), or no change (grey). Marginals along the axes are the one-dimensional distributions for signal and noise at each location (x axis: orange, cued; y axis: blue, uncued). **c.** (Left) Distribution of goodness-of-fit p-values of the m-ADC model to observed responses (randomization test based on the chi-square statistic) for the sham cTBS session. (Right) Same as in the left panel but for stim cTBS session. **d.** Same as in panel (c) but for sham tACS (Left) and stim tACS (Right) sessions. **(e, f)** Same as in panels (c, d), but showing goodness-of-fit p-values comparing the distribution of responses with and without eye-tracking rejection.

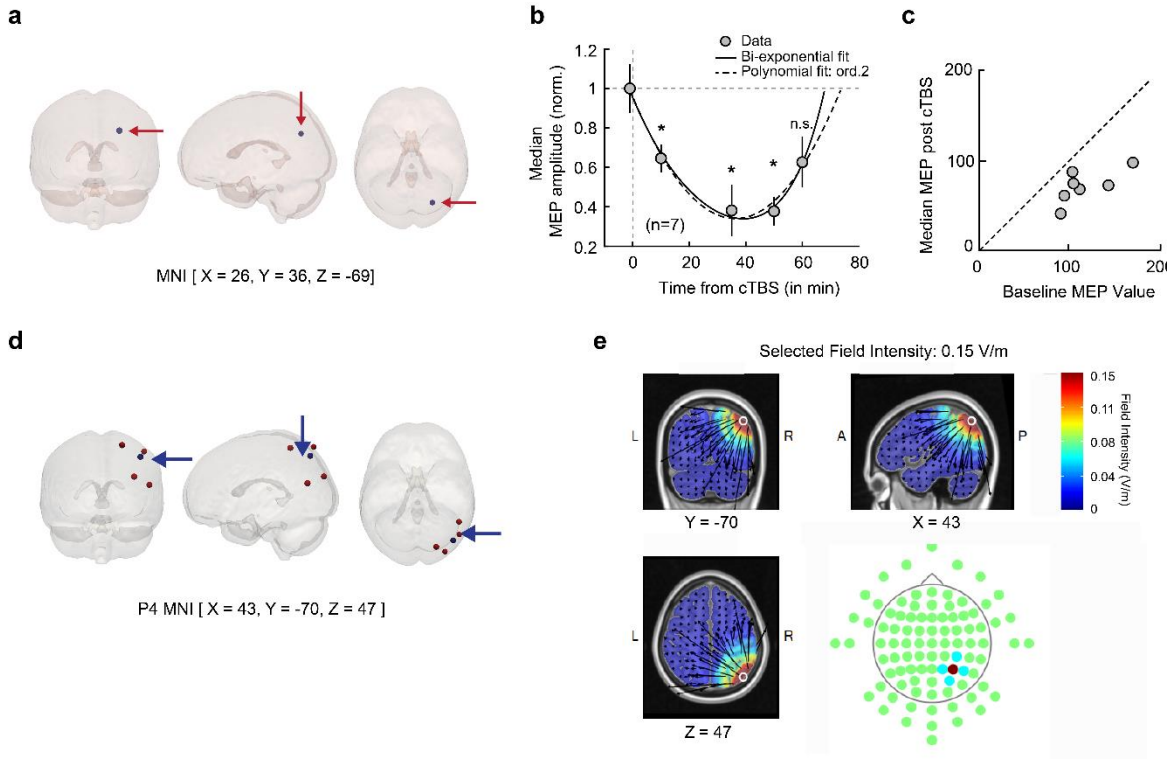

Supplementary Figure S2. Visualization of rPPC stimulation sites, effect of cTBS on motor evoked potential (MEP) amplitude, and visualization of current flow of 40-Hz tACS.

a. Location of the cTBS stimulation site (MNI coordinates: X = 26, Y = 36, Z = -69; blue circle indicated by a red arrow) on coronal, sagittal, and axial sections (left to right) of a glass brain rendering using ITK-SNAP v.3.8.0-beta and ParaView-5.6.0 software. **b.** Median MEP amplitudes measured at several time points following cTBS to the motor cortex (n=7). Dashed vertical line: onset of motor cortex cTBS. Circles: median MEP amplitude across participants at each time point, normalized by the median MEP amplitude measured prior to delivering cTBS. Error bars: s.e.m. Dashed horizontal line: baseline MEP amplitude (normalized). Curved lines: biexponential (solid) and quadratic (dashed) fits. Asterisks: significant difference in MEP amplitude between timepoint and baseline (permutation test; Holm Bonferroni correction for multiple comparisons); n.s.: not significant. The last 2 timepoints (50 min and 60 min) were tested only for 6/7 and 5/7 participants, respectively. **c.** Median MEP amplitudes post cTBS (y axis) plotted against baseline (pre-cTBS) MEP amplitude for the motor cortex cTBS cohort. Circles: individual participants (n=7). Dashed line: line of equality. **d.** Same as in panel (a) but showing the tACS stimulation montage. Electrodes are arranged in a 4x1 high-density montage. Blue circle (indicated by a blue arrow): the 'active' centre electrode placed over P4. Red circles: (four) 'return' electrodes. **e.** Electrical field intensities across coronal (top, left), sagittal (top, right) and axial (bottom, left) views. Stimulation intensity = 1.5 mA peak-to-peak. Black arrows indicate the direction of current flow from the site of stimulation, while colors in the heatmap indicate the current intensity. Bottom right: Site of stimulation showing the locations of anode and cathodes in a 93-electrode model. Red: the 'active' central electrode, here, anode at P4. Blue: 'return' electrodes, here, cathodes at CP4, P6, PO4, P2. During the actual tACS, the anodes and cathodes alternate at the same rate as the frequency of stimulation.

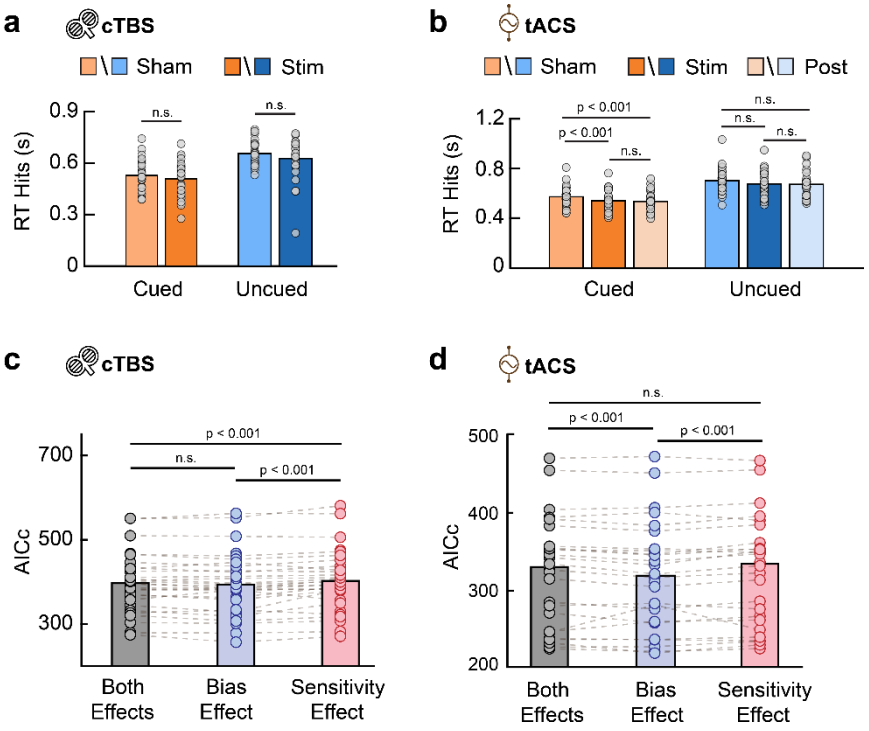

Supplementary Figure S3. Reaction time effects and model comparison analysis using the AICc metric. **a.** Mean reaction times (RT) for reporting change on hit trials at the cued (orange) and uncued (blue) locations during sham and stim cTBS sessions (n=28 participants). Error bars: s.e.m. **b.** Same as in panel (a) but for sham, stim and post tACS sessions (n=26 participants). **c.** Same as in Fig. 3f (main text) but showing the mean AICc values for both effects, bias-effect and sensitivity-effect model for the cTBS cohort. **d.** Same as in panel (c) but for the tACS cohort. **(c, d)** Other conventions are the same as in Fig. 3f.

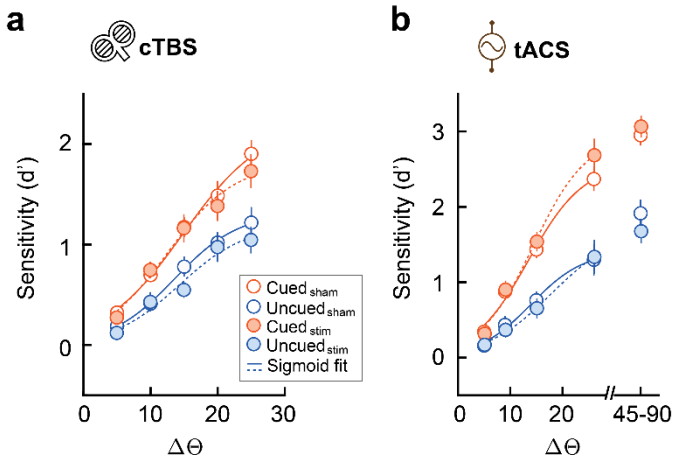

Supplementary Figure S4. Psychophysical functions of sensitivity.
a. Psychophysical function of sensitivity (d') as a function of orientation change angle magnitude (average across n=28 participants) during sham cTBS (open circles) and actual cTBS (filled circles) sessions. Red and blue circles: sensitivity at the cued and uncued locations, respectively. Curves: sigmoid fits. Error bars: s.e.m. **b.** Same as in panel (a) but showing the psychophysical function for sham and actual tACS at 40-Hz (average across n=26 participants). Extreme right: Sensitivities are averaged across the highest change angle magnitudes (45-90°).

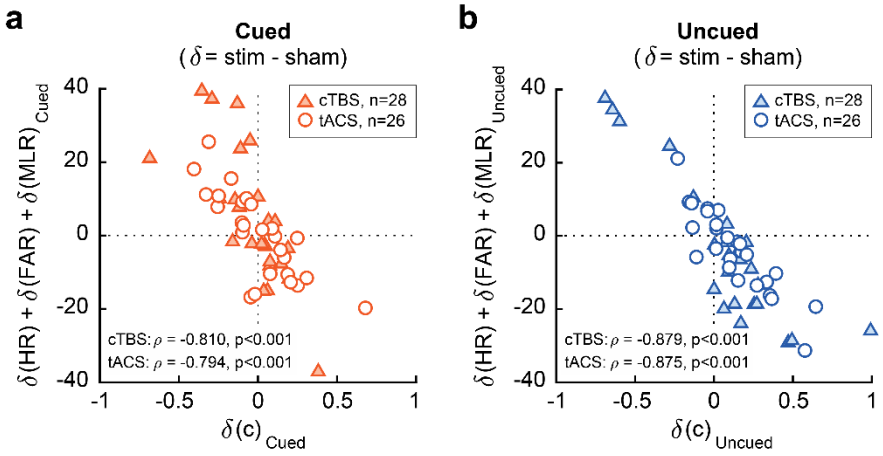

Supplementary Figure S5. Variation of change in criterion with the change in aggregate hit, false alarm and mislocalization responses following stimulation.
a. Scatter plot showing stimulation-induced change in the sum of hit, false alarm and mislocalization rates (δ[HR+FAR+MLR] = [HR+FAR+MLR]$_{stim}$ – [HR+FAR+MLR]$_{sham}$; y-axis) versus stimulation-induced change in criterion ($\delta c = c_{stim} - c_{sham}$; *x*-axis) at the cued location. Filled triangles and open circles: individual participants from the cTBS (n=28) and tACS cohorts (n=26), respectively. **b.** Same as in panel (a) but for the uncued location. Other conventions are the same as in panel (a).

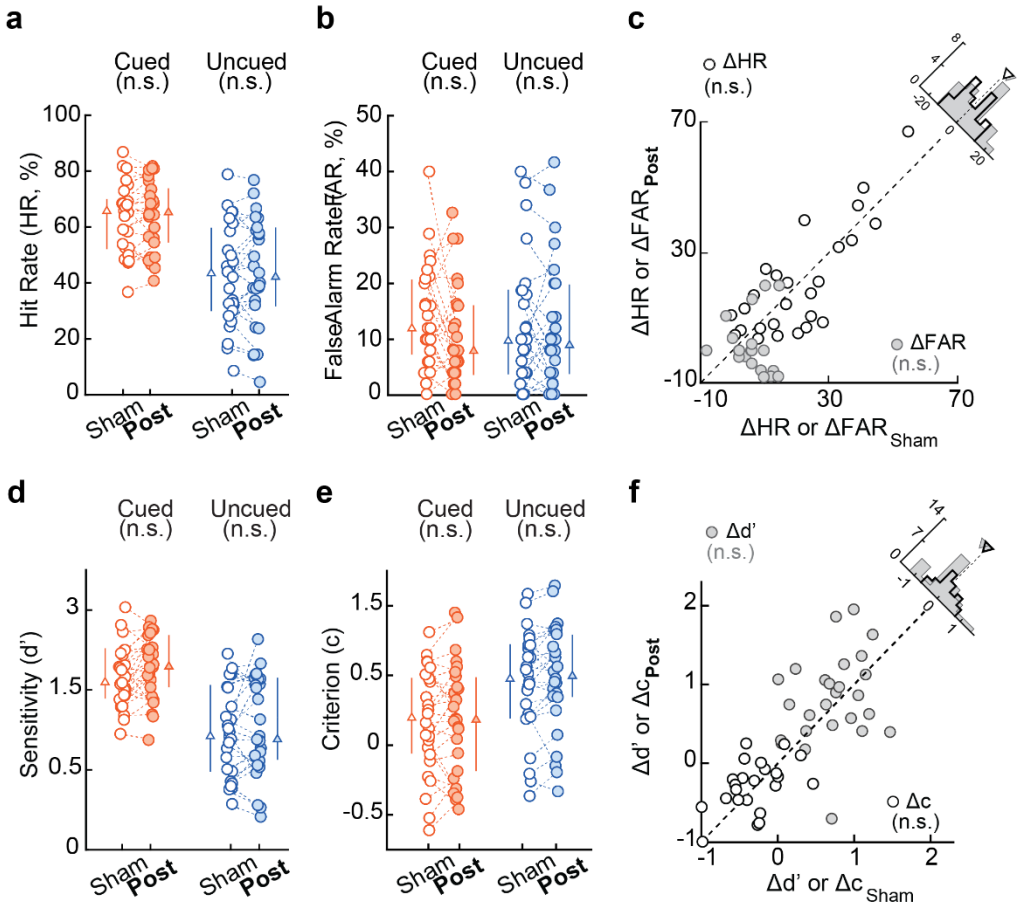

Supplementary Figure S6. Comparison of psychometric and psychophysical parameters across sham and post tACS sessions.

a. Same as in Fig. 4b (main text) but showing Hit Rates (HR) in the sham (open circles) and post (filled circles) tACS sessions (n=26). Other conventions are the same as in Fig. 4b. **b.** Same as in panel (a) but showing False Alarm rates (FAR). **c.** Same as in Fig. 4e (main text) but showing ΔHR (open circles) and ΔFAR (filled grey circles) for sham (*x* axis) and post (*y* axis) tACS sessions. Other conventions are the same as in Fig. 4e. **d.** Same as in Fig. 5a (main text) but showing sensitivity (d') in sham and post tACS sessions. Other conventions are the same as in Fig. 5a. **e**. Same as in panel (d) but showing criterion (c). **f.** Same as in panel (c) but showing Δd' (filled grey circles) and Δc (open circles) during the sham (*x* axis) and post tACS (*y* axis) sessions. Other conventions are the same as in panel (c).

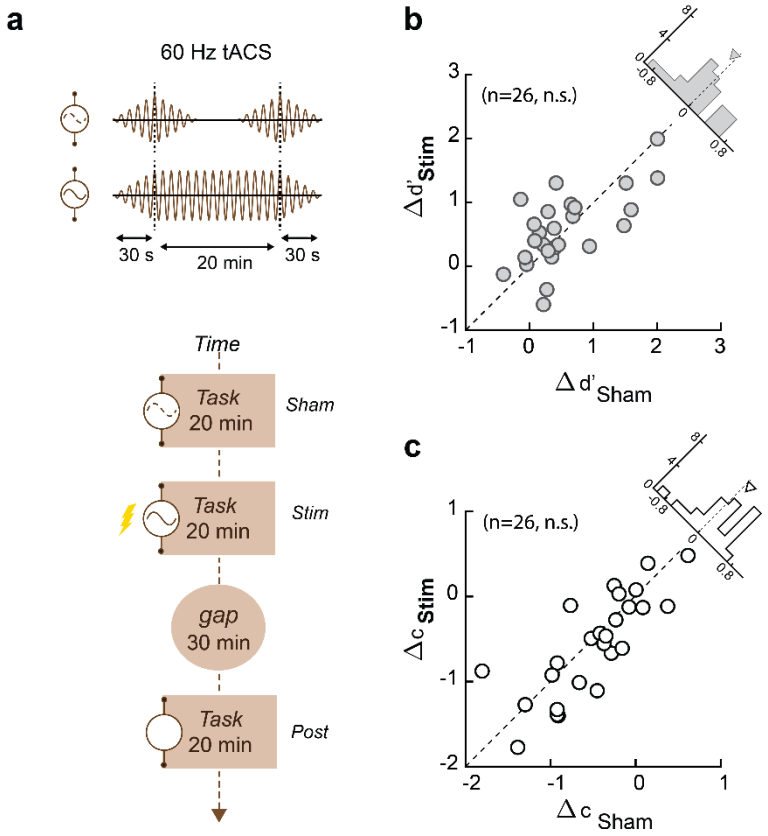

Supplementary Figure S7. Control experiment demonstrating effects of 60-Hz tACS on psychophysical parameters.

a. (Top) Same as in Fig. 1(b, c) (main text) but showing the stimulation and experimental protocols for the control experiment involving 60-Hz tACS over rPPC during the "Stim" session. Other conventions are the same as in Fig. 1(b, c) (tACS panels). **b.** Same as in Fig. 5c (main text) but showing attentional modulation of sensitivity (Δd') for the control experiment (n=26). Other conventions are the same as in Fig. 5c. Data points: individual subjects. **c.** Same as in panel (a) but showing attentional modulation of criterion (Δc) for the control experiment. Other conventions are the same as in panel (b).

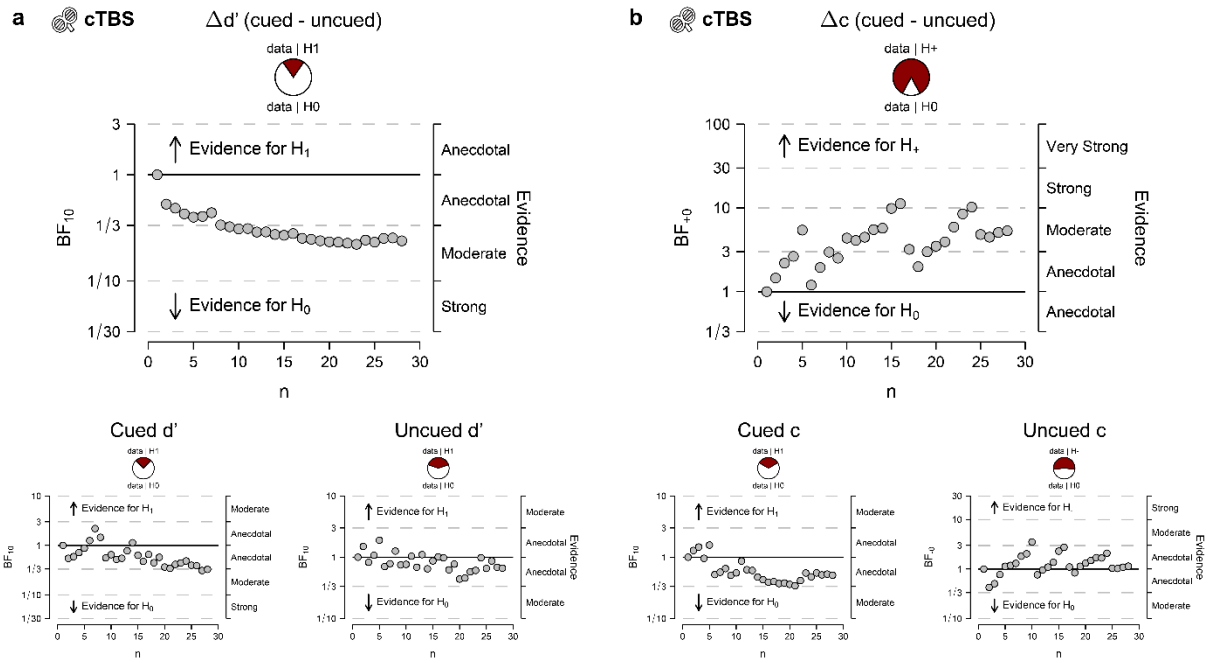

Supplementary Figure S8. Bayesian Paired t-test Sequential Analysis using mADC model estimates of parameters on cTBS cohort.

a. Bayesian T-test Sequential Analysis, as a function of successive data points acquired, for Δd' (top panel) estimated using the mADC model on the cTBS cohort (n=28 participants). Here, H_0 is the hypothesis that Δd' is not different between sham and actual rPPC stimulation sessions. H_1 is the alternative hypothesis that Δd' is different after stimulation. *x*-axis: sequential sample sizes (from n=1 to n=28 participants). Left *y*-axis: Bayesian Factor supporting H_1 over H_0 (BF_{10}). Right *y*-axis: labels for different BF levels. Pie chart: data likelihoods under the two hypotheses. (Bottom panel) Same as the top panel but for d' at the cued (left) and uncued (right) locations. **b**. (Top panel) Same as in panel (a) but for Δc. H+ is the alternative hypothesis that Δc's magnitude increases (i.e., becomes more negative) after stimulation. Left *y*-axis: Bayesian Factor supporting H+ over H_0 (BF_{+0}). (Bottom panel) Same as in panel (a) (bottom) but for c at the cued (left) and uncued (right) locations. (Bottom panel, right) H- is the alternative hypothesis that uncued c increases after stimulation. Left *y*-axis: Bayesian Factor supporting H- over H_0 (BF_{-0}). Other conventions are the same as in panel (a).

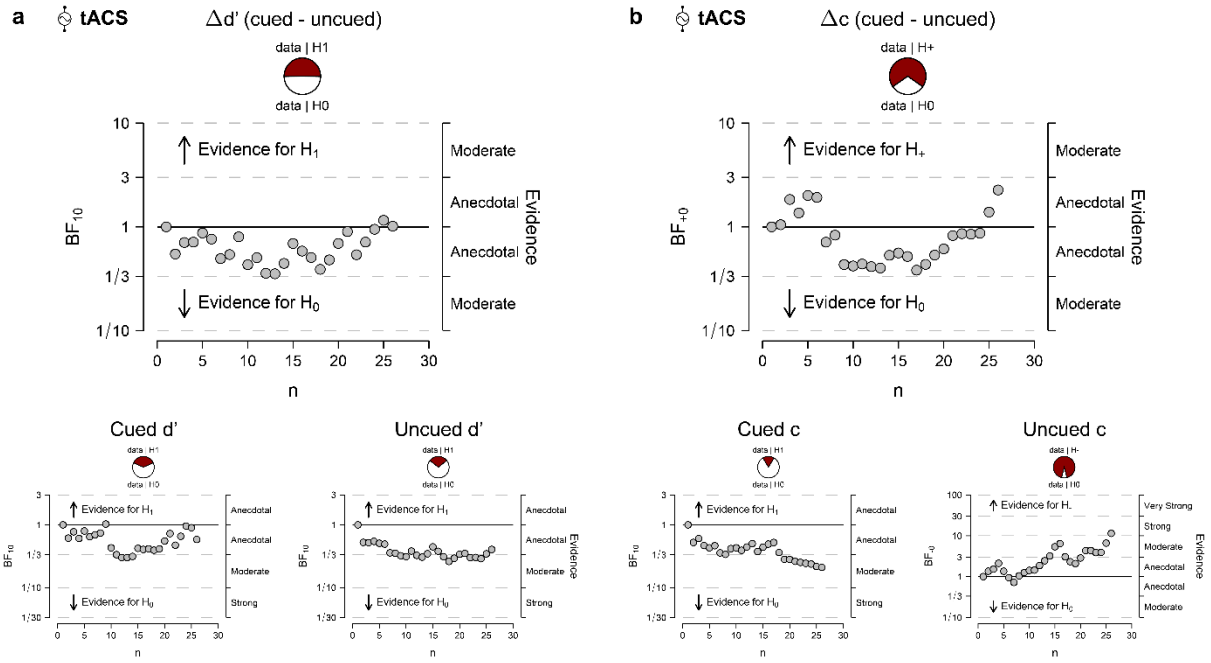

Supplementary Figure S9. Bayesian Paired t-test Sequential Analysis using mADC model estimates of parameters on tACS cohort.

a. Same as in Supplementary Fig. S8a but for Δd' estimated using mADC model on the tACS cohort (n=26 participants). Other conventions are the same as in Supplementary Fig. S8a. **b.** Same as in Supplementary Fig. S8b but for Δc estimated for the tACS cohort. Other conventions are the same as in Supplementary Fig. S8b.

A cTBS Sham session

Change \ Response	Cued	Uncued	No Change
Cued	65.78 ± 3.02	**10.56 ± 1.28**	23.67 ± 2.43
Uncued	**29.48 ± 2.65**	**35.89 ± 2.88**	34.63 ± 2.75
No Change	29.76 ± 3.13	**14.57 ± 1.56**	55.67 ± 3.30

B cTBS Stim session

Change \ Response	Cued	Uncued	No Change
Cued	66.70 ± 3.08	**9.19 ± 1.26** ↓	24.11 ± 2.63
Uncued	**33.73 ± 3.12** ↑	**30.39 ± 3.29** ↓	35.88 ± 3.32
No Change	32.44 ± 3.40	**15.81 ± 2.52** ↑	51.75 ± 3.71

C tACS Sham session

Change \ Response	Cued	Uncued	No Change
Cued	63.28 ± 2.41	**8.14 ± 0.98**	28.57 ± 2.52
Uncued	**12.08 ± 1.69**	**42.68 ± 3.51**	45.24 ± 3.78
No Change	14.21 ± 1.81	**12.78 ± 2.26**	73.01 ± 3.48

D tACS Stim session

Change \ Response	Cued	Uncued	No Change
Cued	64.18 ± 2.31	**6.05 ± 0.93** ↓	29.77 ± 2.59
Uncued	**13.48 ± 1.85** ↑	**38.86 ± 3.71** ↓	47.66 ± 4.42
No Change	12.12 ± 1.81	**14.75 ± 2.14** ↑	73.13 ± 3.67

Supplementary Table S1: **Average stimulus-response contingency tables in the sham and stimulation session. A.** A 3x3 stimulus-response contingency showing the percent (mean ± s.e.m.) of responses for each stimulus event type (cued change, uncued change, and no change) during the sham session in the cTBS cohort (n=28 participants). **B.** Same as in panel A following actual rPPC stimulation in the cTBS cohort. **C.** Same as in panel A but during the sham session in the tACS cohort (n=26 participants). **D.** Same as in panel C following 40-Hz rPPC stimulation in the tACS cohort. **A-D.** Coloured cells and arrows: refer description in SI Results, section on the 'Effects of neurostimulation on mislocalization rates'.